Automatica 169 (2024) 111870

Contents lists available at ScienceDirect

Automatica

journal homepage: www.elsevier.com/locate/automatica

Distributed predefined-time optimal economic dispatch for microgrids☆

Yu Zhang, Yan-Wu Wang, Jiang-Wen Xiao, Xiao-Kang Liu *

School of Artificial Intelligence and Automation, Huazhong University of Science & Technology, Wuhan, 430074, China
Key Laboratory of Image Processing and Intelligent Control, Ministry of Education, Huazhong University of Science and Technology, Wuhan 430074, China

ARTICLE INFO

Article history:
Received 5 November 2023
Received in revised form 21 March 2024
Accepted 2 June 2024
Available online 22 August 2024

Keywords:
Distributed generator
Optimal economic dispatch
Smooth reconstruction penalty method
Distributed predefined-time optimization

ABSTRACT

With the massive popularization of distributed generators, optimal economic dispatch has been a key optimization problem to maintain stable and efficient work of the whole system. In this paper, a new smooth reconstruction penalty function with continuous and piecewise linear differential is designed to deal with generation power constraints, which promotes to obtain a better suboptimal solution compared with the existing smooth penalty methods. A distributed predefined-time optimal economic dispatch strategy is presented by utilizing a time-based function. By employing the proposed strategy, the minimization of the generation cost with transmission loss under the power balance constraint and generation minimum/maximum constraints can be realized within a predefined settling time. The performance of the proposed optimization strategy is evaluated by simulations and hardware-in-the-loop experiments in terms of validity verification, robustness to load change and topology reconfiguration, plug-and-play functionality, and comparison with the existing results to illustrate the advantages of fast convergence and near optimal results.

1. Introduction

As an aggregation of distributed generators (DGs), buses, and loads, microgrid has been studied in recent years to reduce carbon emissions and release environmental pressure (Dragičević et al., 2016; Liu et al., 2023; Schiffer et al., 2016). In a microgrid, optimal economic dispatch, minimizing generation power cost with transmission loss under power balance equality constraint and power generator maximum/minimum inequality constraints, is vital for the stable and efficient operation of the whole system (Li et al., 2019).

To solve the optimal economic dispatch problem, many traditional optimization techniques such as the gradient method, particle swarm algorithm (Gaing, 2003), genetic approach (Chiang, 2005), and approximate dynamic programming strategy (Shuai et al., 2019) are presented. Though with great performance, most of the results are **centralized** optimization strategies. Utilizing a centralized dispatch center to collect global information and send regulation instructions requires a communication infrastructure with high bandwidth and connectivity, which is usually difficult in practical scenarios. Therefore, in Yang et al. (2013), a consensus-based algorithm is designed to solve the economic dispatch problem in a **distributed** method. A distributed optimization strategy is designed based on two consensus algorithms working in parallel to deal with the economic dispatch with transmission loss and generation power constraints in Binetti et al. (2014). A fully distributed control method is presented to achieve optimal resource management through a two-level control framework in Xu and Li (2015). In Binetti et al. (2014), Yang et al. (2013) and Xu and Li (2015), projection operation, **an unsmooth method**, is employed to deal with generation power limits. In Zhao and Ding (2017), a distributed initialization-free optimization approach is raised to address the optimal charging problem of electric vehicles in a microgrid. In Cherukuri and Cortés (2018), a distributed collaborative optimization algorithm is presented to minimize the aggregate cost while meeting the load profile over a weight-balanced strongly connected communication digraph. In Liu et al. (2021), a distributed discrete-time optimal dispatch method is formulated on a weight-unbalanced digraph. In Cherukuri and Cortés (2018), Zhao and Ding (2017) and Liu et al. (2021), exact penalty function

☆ This work is supported by the National Natural Science Foundation of China under Grants 62233006, 62173152 and 62103156, and the Young Elite Scientists Sponsorship Program by CAST (2023QNRC001). The material in this paper was not presented at any conference. This paper was recommended for publication in revised form by Associate Editor Francesco Vasca under the direction of Editor Thomas Parisini.

* Corresponding author at: School of Artificial Intelligence and Automation, Huazhong University of Science & Technology, Wuhan, 430074, China.
E-mail addresses: yuzhang_hust@hust.edu.cn (Y. Zhang), wangyw@hust.edu.cn (Y.-W. Wang), jwxiao@hust.edu.cn (J.-W. Xiao), xiaokangliu@hust.edu.cn (X.-K. Liu).

https://doi.org/10.1016/j.automatica.2024.111870

in **an embedded structure** is exploited to address the inequality constraints in the large-scale optimization problem. However, both the projection operation in Binetti et al. (2014), Yang et al. (2013) and Xu and Li (2015) and the exact penalty function in Cherukuri and Cortés (2018), Zhao and Ding (2017) and Liu et al. (2021) lead to the non-differentiability of the optimization objective, which makes it difficult to gain access to gradient-based optimization techniques and hinders the employment of continuous-time optimization tools.

In low-inertial microgrids, rapid convergence of the power dispatch is beneficial to keep the power balance. In Zhao and Ding (2018), a two-layer optimization strategy is presented by employing a smooth linear-quadratic penalty function to accomplish resource optimization with maintaining the supply–demand balance within a finite time. To realize economic dispatch within a finite time, a distributed consensus-based optimization algorithm is raised in Mao et al. (2021), in which the assumption of the linear increment and boundedness on the gradient of the cost function is relaxed. Under the **finite-time** optimization algorithm in Mao et al. (2021), Zhao and Ding (2018), the convergence time of the power dispatch is dependent on the initial condition, optimization parameters, communication network, and the number of generation units in the microgrid. To overcome the drawbacks, a distributed **fixed-time** optimization algorithm is presented for multi-agent systems with strongly convex cost functions in Wang et al. (2020). An initialization-free distributed power management strategy is raised based on a projection operation or smooth ϵ-exact penalty function in Chen and Guo (2022). A distributed fixed-time cooperative algorithm is proposed to realize both economic dispatch and demand response for generation and load participants within a fixed time in Liu and Yang (2023). Nevertheless, under the distributed fixed-time optimal dispatch strategies in Chen and Guo (2022), Wang et al. (2020) and Liu and Yang (2023), the convergence time of the reference generation power depends on the system communication topology and many optimization parameters, which is not conducive to system deployment. To solve the shortcoming, a **predefined-time** optimal allocation approach is presented by using a smooth linear-quadratic penalty method to give a suboptimal solution within a predefined time in Guo and Chen (2022b). In Guo and Chen (2022a), a distributed dynamic event-triggered optimization strategy is presented by employing projection operator to achieve resource allocation within a predefined time, where the initial condition is constrained. However, the transmission loss is not concerned in Guo and Chen (2022a, 2022b) and the suboptimal solution is far from the optimal solution in Guo and Chen (2022b). Inspired by Shao et al. (2021), a distributed predefined-time optimal economic dispatch strategy based on a smooth reconstruction penalty function is proposed in this paper.

(1) Different from the projection operation in Binetti et al. (2014), Yang et al. (2013) and Xu and Li (2015), the exact penalty function in Cherukuri and Cortés (2018), Zhao and Ding (2017) and Liu et al. (2021), and the smooth linear-quadratic penalty function in Chen and Guo (2022), Zhao and Ding (2018) and Guo and Chen (2022b), a novel smooth reconstruction penalty function is designed with continuous and piecewise linear differential, which promotes to present a better suboptimal power dispatch compared with (Guo & Chen, 2022b).

(2) Compared with the finite-time optimization methods in Mao et al. (2021), Zhao and Ding (2018), the fixed-time optimal dispatch approaches in Chen and Guo (2022), Wang et al. (2020) and Liu and Yang (2023), and the predefined-time economic allocation strategy in Guo and Chen (2022a, 2022b), a distributed predefined-time optimal economic dispatch strategy is proposed to minimize the generation power cost with transmission loss under the power balance equality constraint and generation power minimum/maximum inequality constraints exactly. The power dispatch of DGs can be given within a predefined settling time.

(3) The performance of the proposed optimal economic dispatch strategy is evaluated in numerical simulations and hardware-in-the-loop experiments including validity verification, robustness to load change and topology reconfiguration, and plug-and-play functionality. By comparison with the existing results (Zhao & Ding, 2018), Liu and Yang (2023), and Guo and Chen (2022b), the advantages of fast convergence rate and near optimal results are illustrated.

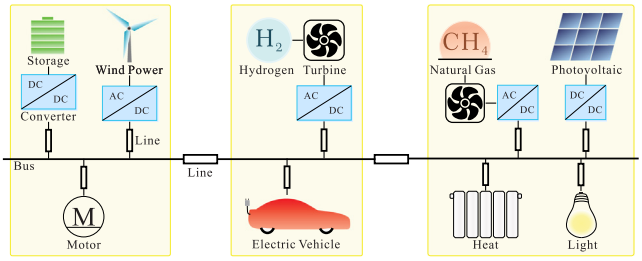

Fig. 1. An illustration of a microgrid.

2. Problem formulation

The microgrid under consideration consists of DGs, converters, and loads, as shown in Fig. 1. A group of distributed various DGs provide reliable power to distributed loads by employing converters, and the transmission lines transmit the power to release pressure on overloaded power nodes and ensure the economic operation of microgrids.

2.1. Optimization goals and communication graph

In a microgrid, optimal economic dispatch problem is to minimize the total generation cost with transmission loss under the power balance equality constraints and the generation power inequality constraints:

$$\min_{P} C_0(P) = \sum_{i=1}^{N} C_i(P_i), \tag{1a}$$

$$\text{s.t.} \sum_{i=1}^{N} P_i = P_L + P_{loss}, \tag{1b}$$

$$P_i^{\text{l}} \le P_i \le P_i^{\text{u}}, i = 1, 2, \ldots, N, \tag{1c}$$

where P_i is the generation power of the ith DG, the generation cost of the DG $C_i(P_i) = a_i P_i^2 + b_i P_i + c_i$, and N is the number of DGs in the microgrid. $P = (P_1, \ldots, P_i, \ldots, P_N)^{\text{T}} \in \mathbb{R}^N$ with $\mathbb{R}^N$ being the set of $N \times 1$ real column vectors. In the power balance constraint ((1)b), the power demand of loads $P_L = \sum_{i=1}^{N} P_{L,i}$ and transmission loss $P_{loss} = \sum_{i=1}^{N} \iota_i P_i + \sum_{i=1}^{N} \iota_{L,i} P_{L,i}$ with ι_i and $\iota_{L,i}$ being the transmission loss coefficients (Xu & Li, 2015). In the generation power constraints ((1)c), P_i^{u} and P_i^{l} are the generation power maximum and minimum bounds, respectively. Therefore, the power balance constraint ((1)b) can be modified as follows:

$$\sum_{i=1}^{N} (1 - \iota_i) P_i = \sum_{i=1}^{N} (1 + \iota_{L,i}) P_{L,i}. \tag{2}$$

In a microgrid, communication graph $\mathcal{G}$ is used to characterize the information interaction. $\mathcal{N}_i$ is the set of neighbors of node i, *i.e.*, if $j \in \mathcal{N}_i$, then node i receives information from node j. $\mathcal{A} = [a_{ij}] \in \mathbb{R}^{N\times N}$ is the adjacency matrix with $\mathbb{R}^{N\times N}$ being the set of $N \times N$ real matrices, where a_{ij} is the communication weight. $a_{ij} > 0$ for $j \in \mathcal{N}_i$ and $a_{ij} = 0$ for $j \notin \mathcal{N}_i$. $\mathcal{D}^{in} = \text{diag}\{d_i^{in}\}$ is a diagonal matrix with $d_i^{in} = \sum_{j\in\mathcal{N}_i} a_{ij}$, and the Laplacian matrix $\mathcal{L} = \mathcal{D}^{in} - \mathcal{A}$.

2.2. Predefined-time optimization

Definition 2.1. (Becerra et al., 2018) Consider a constrained optimization problem:

$$\begin{aligned} &\min f(x) = \sum_{i=1}^{N} f_i(x_i) \\ &\text{s.t.} \sum_{i=1}^{N} x_i = d_0 \\ &\quad g_i(x_i) \le 0, i = 1, 2, \ldots, N, \end{aligned} \tag{3}$$

where $x_i \in \mathbb{R}^N$, $f_i(\cdot)$, $g_i(\cdot) : \mathbb{R}^N \to \mathbb{R}$ and d_0 are the decision variable, the local cost function, the local inequality constraint, and the global equality constraint, respectively. The optimization problem (3) is said to realize predefined-time convergence, if the following conditions hold:

$$\begin{cases} \lim_{t\to t_f} \|x_i - x_i^*\| = 0 \\ \|x_i - x_i^*\| = 0 \ \forall t > t_f \end{cases} \tag{4}$$

where t_f and x_i^* are the predefined time and the optimal decision, respectively. Let $\|x_i - x_i^*\|$ denote the 2-norm of $(x_i - x_i^*) \in \mathbb{R}^N$.

3. Penalty function and suboptimal solution

In this section, a new smooth reconstruction penalty function is designed to deal with the inequality constraints in the optimal economic dispatch problem, and a suboptimal error and condition are derived.

3.1. Optimality without inequality

For the optimization problem (1) without the generation minimum/maximum inequality constraints ((1)c), the Lagrangian function can be presented as follows:

$$\begin{aligned} L &= \sum_{i=1}^{N} C_i(P_i) + \lambda\left(P_L + P_{loss} - \sum_{i=1}^{N} P_i\right) \\ &= \sum_{i=1}^{N}\left(a_i P_i^2 + b_i P_i + c_i\right) \\ &\quad + \lambda\left(\sum_{i=1}^{N}\left(1+\iota_{L,i}\right)P_{L,i} - \sum_{i=1}^{N}(1-\iota_i)P_i\right), \end{aligned} \tag{5}$$

where λ is the Lagrangian multiplier related to the modified power balance constraint (2). To obtain the global optimal solution, let the Lagrangian function with respect to the power and multiplier be 0 as follows.

$$\left.\frac{\partial L}{\partial P_i}\right|_{P_i^*} = \left.\frac{\partial C_i}{\partial P_i}\right|_{P_i^*} - \lambda^*(1-\iota_i) = 0, \tag{6a}$$

$$\left.\frac{\partial L}{\partial \lambda}\right|_{\lambda^*} = \sum_{i=1}^{N}\left(1+\iota_{L,i}\right)P_{L,i} - \sum_{i=1}^{N}(1-\iota_i)P_i^* = 0. \tag{6b}$$

From (6), the global optimal solution without generation power limits is shown as follows.

$$P_i^* = \frac{\lambda^*(1-\iota_i) - b_i}{2a_i}, \tag{7a}$$

$$\lambda^* = \frac{P_D + \sum_{i=1}^{N}\frac{(1-\iota_i)b_i}{2a_i}}{\sum_{i=1}^{N}\frac{(1-\iota_i)^2}{2a_i}}, \tag{7b}$$

where $P_D = \sum_{i=1}^{N}\left(1+\iota_{L,i}\right)P_{L,i}$.

Considering the generation power minimum and maximum inequality constraints ((1)c), the necessary conditions for the optimization problem can be expanded slightly as follows (Wood et al., 2013).

$$\begin{cases} \frac{1}{1-\iota_i}\frac{\partial C_i}{\partial P_i} = \lambda^*, & P_i^{\text{l}} \le P_i \le P_i^{\text{u}} \\ \frac{1}{1-\iota_i}\frac{\partial C_i}{\partial P_i} \ge \lambda^*, & P_i = P_i^{\text{l}} \\ \frac{1}{1-\iota_i}\frac{\partial C_i}{\partial P_i} \le \lambda^*, & P_i = P_i^{\text{u}} \end{cases} \tag{8}$$

3.2. Suboptimality with inequality

In a microgrid, it is necessary for the stable work of DGs to generate power within the generation maximum and minimum limits. To deal with the generation constraints, a novel smooth reconstruction penalty function $p_{\epsilon,i}(P_i)$ is designed as follows

$$p_{\epsilon,i}(P_i) = \begin{cases} 0, & h_i(P_i) \le 0 \\ \frac{k_\epsilon}{2}h_i^{\text{u}}(P_i), & 0 < h_i(P_i) \le \epsilon_i, P_i > P_i^{\text{u}} \\ \frac{k_\epsilon}{2}h_i^{\text{l}}(P_i), & 0 < h_i(P_i) \le \epsilon_i, P_i < P_i^{\text{l}} \\ h_i(P_i) - \frac{\epsilon_i - \Delta\epsilon_i^2}{2}, & h_i(P_i) > \epsilon_i \end{cases} \tag{9}$$

where $h_i(P_i) = (P_i^{\text{l}} - P_i)(P_i^{\text{u}} - P_i)$, $h_i^{\text{u}}(P_i) = \left(P_i^{\text{u}} - P_i\right)^2$ and $h_i^{\text{l}}(P_i) = \left(P_i^{\text{l}} - P_i\right)^2$. $\epsilon_i = h_i\left(P_i^{\text{u}} + \Delta\epsilon_i\right) = (1+\tau)\tau P_i^{\text{ul}^2}$ with $\Delta\epsilon_i = \tau P_i^{\text{ul}}$ and $P_i^{\text{ul}} = P_i^{\text{u}} - P_i^{\text{l}}$. τ is a positive scalar that regulates optimization error, and $k_\epsilon = \frac{P_i^{\text{ul}} + 2\Delta\epsilon_i}{\Delta\epsilon_i} = \frac{1+2\tau}{\tau}$. Thus,

$$\frac{\partial p_{\epsilon,i}}{\partial P_i} = \begin{cases} 0, & h_i(P_i) \le 0 \\ k_\epsilon\left(P_i - P_i^{\text{u}}\right), & 0 < h_i(P_i) \le \epsilon_i, P_i > P_i^{\text{u}} \\ k_\epsilon\left(P_i - P_i^{\text{l}}\right), & 0 < h_i(P_i) \le \epsilon_i, P_i < P_i^{\text{l}} \\ 2P_i - P_i^{\text{u}} - P_i^{\text{l}}, & h_i(P_i) > \epsilon_i \end{cases} \tag{10}$$

Remark 3.1. Different from the smooth linear-quadratic penalty function in Chen and Guo (2022), Zhao and Ding (2018) and Guo and Chen (2022b), the proposed smooth penalty function (9) is reconstructed based on the decision function $h_i(P_i)$ in the range of $h_i(P_i) \in (0, \epsilon_i]$, which turns the differential of the penalty function (10) into a piecewise linear function. Based on the proposed penalty function, the order of cost function gradient is reduced compared with those in Guo and Chen (2022b), Zhao and Ding (2018) and Pinar and Zenios (1994).

As an extension of ϵ-feasibility in Guo and Chen (2022b), Zhao and Ding (2018) and Pinar and Zenios (1994), $\Delta\epsilon$-feasibility is given as follows.

Definition 3.1. $\tilde{P} = (\tilde{P}_1, \ldots, \tilde{P}_i)^{\text{T}}$ is defined to be $\Delta\epsilon$-feasible, if $P_i^{\text{l}} - \Delta\epsilon_i \le \tilde{P}_i \le P_i^{\text{u}} + \Delta\epsilon_i, i = 1, \ldots, N$.

By employing the smooth reconstruction penalty function (9), the objective function is reconstructed as follows,

$$C_\epsilon(P) = \sum_{i=1}^{N} C_{\epsilon,i}(P_i) = \sum_{i=1}^{N} C_i(P_i) + \mu p_{\epsilon,i}(P_i), \tag{11}$$

where the Lagrange multiplier μ is a positive constant to regulate the severity of the penalty function. Let $P_\epsilon^* = (P_{\epsilon,1}^*, \ldots, P_{\epsilon,N}^*)^{\mathrm{T}}$ be a $\Delta\epsilon$-feasible suboptimal solution of (11). In the following, the optimization error between the real optimal solution and the suboptimal solution P_ϵ^* caused by the proposed penalty function will be discussed.

Lemma 3.1. *For the optimal solution P_e^* and the $\Delta\epsilon$-feasible suboptimal solution P_ϵ^*,*

$$0 \le C_0\left(P_e^*\right) - C_0\left(P_\epsilon^*\right) \le \mu\epsilon_s, \tag{12}$$

where $\epsilon_s = \sum_{i=1}^N \epsilon_i$.

Proof. To obtain the optimization error, an exact penalty function $p_i(P_i)$ is introduced (Bertsekas, 1975):

$$p_i(P_i) = \begin{cases} 0, & h_i(P_i) \le 0 \\ h_i(P_i), & h_i(P_i) > 0 \end{cases} \tag{13}$$

The objective function for the exact penalty $p_i(P_i)$ is formulated as:

$$C_e(P) = \sum_{i=1}^N C_{e,i}(P_i) = \sum_{i=1}^N C_i(P_i) + \mu p_i(P_i). \tag{14}$$

Denote $P_e^* = (P_{e,1}^*, \ldots, P_{e,N}^*)^{\mathrm{T}}$ as an optimal solution of (14). P_e^* is the optimal solution if $\mu = \mu^* > \max\{\mu_i^s\}$ with $\mu^s = (\mu_1^s, \ldots, \mu_N^s)^{\mathrm{T}}$ being the Lagrange multiplier satisfying the KKT condition (Bertsekas, 1975; Pinar & Zenios, 1994). The upper bound of μ^s is given as follows (Kia, 2016).

$$\max\left\{\mu_i^s\right\} < \frac{2\max\left\{\max_{P_i\in\mathbb{P}_i}\left\{\frac{\partial C_i}{\partial P_i}\right\}\right\}}{\min\left\{P_i^{\mathrm{u}} - P_i^{\mathrm{l}}\right\}}, \tag{15}$$

where the generation power feasible set for the ith DGs $\mathbb{P}_i = \{P_i \in \mathbb{R} | \, h_i(P_i) \le 0, \sum_{i=1}^N (1-\iota_i)P_i = \sum_{i=1}^N (1+\iota_{L,i})P_{L,i}\}$.

From the definition of $p_{\epsilon,i}(P_i)$ in (9) and $p_i(P_i)$ in (13),

$$0 \le p_i(P_i) - p_{\epsilon,i}(P_i) \le \frac{\epsilon_i - \Delta\epsilon_i^2}{2}. \tag{16}$$

Together with (11) and (14),

$$0 \le C_{e,i}(P_i) - C_{\epsilon,i}(P_i) \le \frac{\mu\tau}{2}P_i^{\mathrm{ul}2}. \tag{17}$$

Taking the infimum of (17) gives

$$0 \le C_{e,i}\left(P_{e,i}^*\right) - C_{\epsilon,i}\left(P_{\epsilon,i}^*\right) \le \frac{\mu\tau}{2}P_i^{\mathrm{ul}2}. \tag{18}$$

Recall that P_e^* is an optimal solution,

$$p_{e,i}(P_{e,i}^*) = 0, \tag{19}$$

and P_ϵ^* is $\Delta\epsilon$-feasible,

$$0 \le p_{\epsilon,i}\left(P_{\epsilon,i}^*\right) \le \frac{(1+2\tau)\tau}{2}P_i^{\mathrm{ul}2}. \tag{20}$$

From (11), (14), and (18),

$$\begin{aligned} 0 \le &\sum_{i=1}^N C_i\left(P_{e,i}^*\right) + \sum_{i=1}^N \mu p_{e,i}\left(P_{e,i}^*\right) - \sum_{i=1}^N C_i\left(P_{\epsilon,i}^*\right) \\ &- \sum_{i=1}^N \mu p_{\epsilon,i}\left(P_{\epsilon,i}^*\right) \le \sum_{i=1}^N \frac{\mu\tau}{2}P_i^{\mathrm{ul}2}. \end{aligned} \tag{21}$$

Substituting (19) and (20) into (21), the result is obtained. □

After obtaining an upper bound on the optimization error incurred by $p_{\epsilon,i}$ instead of p_i, the threshold of μ for $\Delta\epsilon$-feasibility is characterized.

Lemma 3.2. *P_ϵ^* satisfies $\Delta\epsilon$-feasibility if μ is given as follows*

$$\mu = \frac{\mu^*}{\kappa_\epsilon}. \tag{22}$$

where the multiplier gain κ_ϵ is chosen by

$$\kappa_\epsilon = \frac{1}{\frac{\sqrt{P_N^{\mathrm{ul}}+1}}{1+2\tau} + 1}, \tag{23}$$

with $P_N^{\mathrm{ul}} = (N-1)\frac{\overline{P}^{\mathrm{ul}2}}{\underline{P}^{\mathrm{ul}2}}$, $\underline{P}^{\mathrm{ul}} = \min\{P_i^{\mathrm{ul}}\}$ and $\overline{P}^{\mathrm{ul}} = \max\{P_i^{\mathrm{ul}}\}$.

Proof. Denote $\mathbb{P}_w$ and $\mathbb{P}_b$ as the sets of indices corresponding to constraints which are satisfied within $\Delta\epsilon_i$ at P_ϵ^* and violated beyond $\Delta\epsilon_i$ at P_ϵ^*. Assume that the cardinality of $\mathbb{P}_b$ is at least one. The following analysis is conducted by contradiction. The objective function with the smooth reconstruction penalty term is written as follows

$$\begin{aligned} C_\epsilon(P_\epsilon^*) = &\sum_{i=1}^N C_i(P_{\epsilon,i}^*) + \mu\sum_{i\in\mathbb{P}_b}\left(h_i(P_{\epsilon,i}^*) - \frac{\epsilon_i - \Delta\epsilon_i^2}{2}\right) \\ &+ \mu\sum_{i\in\mathbb{P}_w}\frac{k_\epsilon}{2}h_i^{\mathrm{u}}(P_{\epsilon,i}^*). \end{aligned} \tag{24}$$

Note that the penalty function $p_{\epsilon,i}(P_i)$ is symmetric about $\frac{P_i^{\mathrm{u}}+P_i^{\mathrm{l}}}{2}$, so only the case of $P_i^{\mathrm{u}} < P_{\epsilon,i}^* \le P_i^{\mathrm{u}} + \Delta\epsilon_i$ will be analyzed.

(1) For the 2nd term in (24),

$$\begin{aligned} &\mu\sum_{i\in\mathbb{P}_b}(h_i(P_{\epsilon,i}^*) - \frac{\epsilon_i - \Delta\epsilon_i^2}{2}) = \mu^*\sum_{i\in\mathbb{P}_b}h_i(P_{\epsilon,i}^*) \\ &+ \left(\mu\sum_{i\in\mathbb{P}_b}(h_i(P_{\epsilon,i}^*) - \frac{\epsilon_i - \Delta\epsilon_i^2}{2}) - \mu^*\sum_{i\in\mathbb{P}_b}h_i(P_{\epsilon,i}^*)\right) \\ &= \mu^*\sum_{i\in\mathbb{P}_b}h_i(P_{\epsilon,i}^*) + \mu^*\sum_{i\in\mathbb{P}_b}h_{b,i}^{\epsilon\kappa}(P_{\epsilon,i}^*) \end{aligned} \tag{25}$$

where $h_{b,i}^{\epsilon\kappa}(P_{\epsilon,i}^*) = \frac{h_i(P_{\epsilon,i}^*) - \frac{\epsilon_i - \Delta\epsilon_i^2}{2}}{\kappa_\epsilon} - h_i(P_{\epsilon,i}^*)$. From the definition of κ_ϵ and $\tau \ll 1$, we have $0 < \kappa_\epsilon < \frac{1}{2}$. For $h_i(P_{\epsilon,i}^*) > \epsilon_i$,

$$h_{b,i}^{\epsilon\kappa}(P_{\epsilon,i}^*) > \frac{\epsilon_i + \Delta\epsilon_i^2}{2\kappa_\epsilon} - \epsilon_i. \tag{26}$$

From (25) and (26), then

$$\mu\sum_{i\in\mathbb{P}_b}(h_i(P_{\epsilon,i}^*) - \frac{\epsilon_i - \Delta\epsilon_i^2}{2}) > \mu^*\sum_{i\in\mathbb{P}_b}h_i(P_{\epsilon,i}^*) + \mu^* h_b^*, \tag{27}$$

where $h_b^* = \min\{\frac{\epsilon_i + \Delta\epsilon_i^2}{2\kappa_\epsilon} - \epsilon_i\} = (\frac{(1+2\tau)\tau}{2\kappa_\epsilon} - (1+\tau)\tau)\underline{P}^{\mathrm{ul}2}$.

(2) For the 3rd term in (24),

$$\begin{aligned} &\mu\sum_{i\in\mathbb{P}_w}\frac{k_\epsilon}{2}h_i^{\mathrm{u}}(P_{\epsilon,i}^*) = \mu^*\sum_{i\in\mathbb{P}_w}h_i(P_{\epsilon,i}^*) \\ &+ \left(\mu\sum_{i\in\mathbb{P}_w}\frac{k_\epsilon}{2}h_i^{\mathrm{u}}(P_{\epsilon,i}^*) - \mu^*\sum_{i\in\mathbb{P}_w}h_i(P_{\epsilon,i}^*)\right) \\ &= \mu^*\sum_{i\in\mathbb{P}_w}h_i(P_{\epsilon,i}^*) + \mu^*\left(\sum_{i\in\mathbb{P}_w}h_{w,i}^{\epsilon\kappa}(P_{\epsilon,i}^*)\right), \end{aligned} \tag{28}$$

where $h^{\epsilon\kappa}_{w,i}(P^*_{\epsilon,i}) = (P^{\mathrm{u}}_i - P^*_{\epsilon,i})(k_{\epsilon\kappa}(P^{\mathrm{u}}_i - P^*_{\epsilon,i}) - (P^{\mathrm{l}}_i - P^*_{\epsilon,i}))$ with $k_{\epsilon\kappa} = \frac{k_\epsilon}{2\kappa_\epsilon}$.

$$\begin{aligned}\frac{dh^{\epsilon\kappa}_{w,i}}{dP^*_{\epsilon,i}} &= (P^{\mathrm{l}}_i - P^*_{\epsilon,i}) + (P^{\mathrm{u}}_i - P^*_{\epsilon,i})(1-2k_{\epsilon\kappa}) \\ &= 2(k_{\epsilon\kappa}-1)P^*_{\epsilon,i} + 2(1-k_{\epsilon\kappa})P^{\mathrm{u}}_i - P^{\mathrm{ul}}_i.\end{aligned} \tag{29}$$

The minimum of $h^{\epsilon\kappa}_{w,i}(P^*_{\epsilon,i})$ is attained at $P^{\mathrm{m},*}_{\epsilon,i} = P^{\mathrm{u}}_i + \frac{P^{\mathrm{ul}}_i}{2(k_{\epsilon\kappa}-1)}$. Recall $0 < \kappa_\epsilon < \frac{1}{2}$, then $P^{\mathrm{u}}_i < P^{\mathrm{m},*}_{\epsilon,i} = P^{\mathrm{u}}_i + \frac{\kappa_\epsilon \Delta\epsilon_i}{1+2\tau(1-\kappa_\epsilon)} < P^{\mathrm{u}}_i + \Delta\epsilon_i$. At the point of $P^{\mathrm{m},*}_{\epsilon,i}$,

$$h^{\epsilon\kappa}_{w,i}(P^{\mathrm{m},*}_{\epsilon,i}) = -\frac{\kappa_\epsilon \tau}{2(1+2\tau(1-\kappa_\epsilon))}P^{\mathrm{ul}2}_i. \tag{30}$$

From (28) and (30),

$$\mu \sum_{i\in\mathbb{P}_w} \frac{k_\epsilon}{2} h^{\mathrm{u}}_i(P^*_{\epsilon,i}) \geq \mu^* \sum_{i\in\mathbb{P}_w} h_i(P^*_{\epsilon,i}) + \mu^*(N-1)h^*_w, \tag{31}$$

where $h^*_w = -\frac{\kappa_\epsilon \tau}{2(1+2\tau(1-\kappa_\epsilon))}\overline{P}^{\mathrm{ul}2}$.

Combine (24), (27), and (31), then

$$\begin{aligned}C_\epsilon(P^*_\epsilon) > &\sum_{i=1}^N C_i(P^*_{\epsilon,i}) + \mu^* \sum_{i\in\mathbb{P}_b} h_i(P^*_{\epsilon,i}) + \mu^* h^*_b \\ &+ \mu^* \sum_{i\in\mathbb{P}_w} h_i(P^*_{\epsilon,i}) + \mu^*(N-1)h^*_w,\end{aligned} \tag{32}$$

By the definition of κ_ϵ in (23),

$$h^*_b + (N-1)h^*_w = 0. \tag{33}$$

Then,

$$\begin{aligned}C_\epsilon(P^*_\epsilon) &> \sum_{i=1}^N C_i(P^*_{\epsilon,i}) + \mu^* \sum_{i=1}^N p_i(P^*_{\epsilon,i}) \\ &\geq \sum_{i=1}^N C_i(P^*_{e,i}) + \mu^* \sum_{i=1}^N p_i(P^*_{e,i}).\end{aligned} \tag{34}$$

which contradicts (18). Hence, under (22)–(23), the set $\mathbb{P}_b$ must be empty, which means P^*_ϵ is $\Delta\epsilon$-feasible. □

Note that $\Delta\epsilon_i$ can be made arbitrarily small by choosing small enough τ. Thus, the $\Delta\epsilon$-feasible suboptimal solution does not hinder the stable work of the DGs.

Remark 3.2. From (12) and (22), the upper bound of the optimization error can be formulated as follows.

$$\begin{aligned}\mu\epsilon_s &= \left(\frac{\sqrt{P^{\mathrm{ul}}_N + 1}}{1+2\tau} + 1\right)\mu^*(1+\tau)\tau \sum_{i=1}^N P^{\mathrm{ul}2}_i \\ &= \left(\frac{\sqrt{P^{\mathrm{ul}}_N + 1}}{\frac{1}{\tau} + \frac{1}{1+\tau}} + (1+\tau)\tau\right)\mu^* \sum_{i=1}^N P^{\mathrm{ul}2}_i.\end{aligned}$$

Thus, the optimization error can be decreased by reducing the adjustable parameter τ.

Based on Lemmas 3.1 and 3.2, the optimization problem (1) can be further presented as

$$\min_{P_i} \sum_{i=1}^N C_{\epsilon,i}(P_i), \tag{35a}$$

$$\text{s.t.} \sum_{i=1}^N (1-\iota_i)P_i = \sum_{i=1}^N (1+\iota_{L,i})P_{L,i}, \tag{35b}$$

and the suboptimal condition for (35) is given as follows

$$\nabla C_{\epsilon,i}\left(P^*_{\epsilon,i}\right) = \lambda^*_\epsilon, \tag{36a}$$

$$\sum_{i=1}^N \left(1+\iota_{L,i}\right)P_{L,i} = \sum_{i=1}^N (1-\iota_i)P^*_{\epsilon,i}. \tag{36b}$$

where $\nabla C_{\epsilon,i}\left(P^*_{\epsilon,i}\right) = \frac{1}{\bar{\iota}_i}\frac{\partial C_{\epsilon,i}}{\partial P_i}\Big|_{P^*_{\epsilon,i}}$ is the modified gradient with $\bar{\iota}_i = 1-\iota_i$. From (10) and (11),

$$(\nabla C_{\epsilon,i}(P_i) - \nabla C_{\epsilon,i}(P^*_{\epsilon,i}))(P_i - P^*_{\epsilon,i}) \geq \frac{2a_i}{\bar{\iota}_i}(P_i - P^*_{\epsilon,i})^2, \tag{37a}$$

$$\left|\nabla C_{\epsilon,i}(P_i) - \nabla C_{\epsilon,i}\left(P^*_{\epsilon,i}\right)\right| \leq \frac{2(a_i+\mu)+\frac{\mu}{\tau}}{\bar{\iota}_i}\left|P_i - P^*_{\epsilon,i}\right|. \tag{37b}$$

Remark 3.3. Different from the exact penalty (13), the penalty function (9) is continuously differentiable, which makes gradient-based optimization techniques available. Compared with the smooth linear-quadratic penalty method in Pinar and Zenios (1994), Zhao and Ding (2018) and Guo and Chen (2022b), the piecewise linear smooth reconstruction penalty function differential (10) can effectively reduce the order of the cost function gradient. Moreover, the introduction of τ to ϵ_i in (9) generates a variable $\Delta\epsilon_i$ feasible set with the optimization error being $\mu\sum_{i=1}^N \epsilon_i$ instead of the constant ϵ feasible set with the optimization error being $(1+\sqrt{N})\mu^* N\epsilon$ in Pinar and Zenios (1994), Zhao and Ding (2018) and Guo and Chen (2022b). To compare the optimization error under the proposed penalty function and the linear-quadratic penalty function, the relationship between ϵ_i in (9) and ϵ in Pinar and Zenios (1994), Zhao and Ding (2018) and Guo and Chen (2022b) is given as $\epsilon = \max\{\epsilon_i\}$, which means the same feasible set for the key DG. Then, when the parameter τ satisfies the following condition:

$$\tau \geq \frac{\sqrt{P^{\mathrm{ul}}_N + 1}}{(1+\sqrt{N})\frac{2N\overline{P}^{\mathrm{ul}2}}{\sum_{i=1}^N P^{\mathrm{ul}2}_i} - 2} - \frac{1}{2},$$

there exists $\mu\sum_{i=1}^N \epsilon_i \leq (1+\sqrt{N})\mu^* N\epsilon$ which means that the optimization error can be decreased by employing the smooth reconstruction penalty function (9).

4. Distributed predefined-time optimization strategy

In the following, a distributed predefined-time strategy is designed to achieve the optimal economic dispatch with transmission loss under power balance and generation constraints within a predefined settling time.

$$\dot{P}^r_i = \frac{\omega(t)}{\bar{\iota}_i}\left(-\nabla C_{\epsilon,i}\left(P^r_i\right) + \bar{\iota}_i\xi_i\right), \tag{38a}$$

$$\dot{\xi}_i = \frac{\omega(t)}{\bar{\iota}_i}\left(-e^\xi_i - e^\nu_i + P^m_i\right), \tag{38b}$$

$$\dot{\nu}_i = \frac{\omega(t)}{\bar{\iota}_i}e^\xi_i, \tag{38c}$$

where P^r_i is the reference generation power. The local power mismatch $P^m_i = (1+\iota_{L,i})P_{L,i} - \bar{\iota}_i P^r_i$. ξ_i and ν_i are auxiliary variables with $e^\xi_i = \sum_{j\in\mathcal{N}_i} a_{ij}\left(\bar{\iota}_i\xi_i - \bar{\iota}_j\xi_j\right)$ and $e^\nu_i = \sum_{j\in\mathcal{N}_i} a_{ij}\left(\bar{\iota}_i\nu_i - \bar{\iota}_j\nu_j\right)$. Motivated by Shao et al. (2021), the time-based gain $\omega(t)$ is designed as $\omega(t) = r_1 + \frac{r_2}{t_a}\Omega(t)$, where $\Omega(t) = \begin{cases}\frac{t_a}{t_a - t}, & t\in[0,t_a)\\ 1, & t\in[t_a,+\infty)\end{cases}$ and $\dot{\Omega}(t) = \begin{cases}\frac{1}{t_a}\Omega(t)^2, & t\in[0,t_a)\\ 0, & t\in[t_a,+\infty)\end{cases}$.

Theorem 4.1. *For an undirected and connected communication graph $\mathcal{G}$, the reference generation power P_i^r in (38) converges to the $\Delta\epsilon$-feasible suboptimal solution $P_{\epsilon,i}^*$ within the predefined settling time t_a.*

Proof. The proposed distributed optimization strategy (38) can be given in a compact form as follows.

$$\bar{\iota}\dot{P}^r = \omega(t)\left(-\nabla C_\epsilon\left(P^r\right) + \bar{\iota}\xi\right), \tag{39a}$$

$$\bar{\iota}\dot{\xi} = \omega(t)\left(-\mathcal{L}\bar{\iota}\xi - \mathcal{L}\bar{\iota}\nu + P^m\right), \tag{39b}$$

$$\bar{\iota}\dot{\nu} = \omega(t)\mathcal{L}\bar{\iota}\xi, \tag{39c}$$

where $\bar{\iota} = \mathrm{diag}\{\bar{\iota}_1, \ldots, \bar{\iota}_N\}$, $P^r = (P_1^r, \ldots, P_N^r)^{\mathrm{T}}$, $\xi = (\xi_1, \ldots, \xi_N)^{\mathrm{T}}$, $\nu = (\nu_1, \ldots, \nu_N)^{\mathrm{T}}$, and $P^m = (P_1^m, \ldots, P_N^m)^{\mathrm{T}}$. Let P^{rs}, P^{ms}, ξ^{s}, and ν^{s} denote the equilibrium point of (39), then

$$0 = \omega(t)\left(-\nabla C_\epsilon\left(P^{rs}\right) + \bar{\iota}\xi^{\mathrm{s}}\right), \tag{40a}$$

$$0 = \omega(t)\left(-\mathcal{L}\bar{\iota}\xi^{\mathrm{s}} - \mathcal{L}\bar{\iota}\nu^{\mathrm{s}} + P^{ms}\right), \tag{40b}$$

$$0 = \omega(t)\mathcal{L}\bar{\iota}\xi^{\mathrm{s}}. \tag{40c}$$

Left-multiply ((40)b) by $1_N^{\mathrm{T}} = (1, \ldots, 1) \in \mathbb{R}^{1\times N}$, then

$$1_N^{\mathrm{T}} P^{ms} = 0. \tag{41}$$

Together with ((40)a) and ((40)c), we have $\nabla C_\epsilon(P_i^{rs}) = \nabla C_\epsilon(P_j^{rs})$, $\forall i, j = 1, \ldots, N$. To analyze the predefined-time stability of the distributed optimization strategy (38), let $\tilde{P} = \bar{\iota}P^r - \bar{\iota}P^{rs}$, $g = \nabla C_\epsilon\left(P^r\right) - \nabla C_\epsilon\left(P^{rs}\right)$, $\tilde{\xi} = \bar{\iota}\xi - \bar{\iota}\xi^{\mathrm{s}}$, and $\tilde{\nu} = \bar{\iota}\nu - \bar{\iota}\nu^{\mathrm{s}}$ denote the error variables. Then,

$$\dot{\tilde{P}} = \omega(t)(-g + \tilde{\xi}), \tag{42a}$$

$$\dot{\tilde{\xi}} = \omega(t)\left(-\mathcal{L}\tilde{\xi} - \mathcal{L}\tilde{\nu} - \tilde{P}\right), \tag{42b}$$

$$\dot{\tilde{\nu}} = \omega(t)\mathcal{L}\tilde{\xi}. \tag{42c}$$

It is obvious that there exists an orthogonal matrix $T = [T_1, T_{-1}]^{\mathrm{T}}$ to ensure $\mathcal{L} = T^{\mathrm{T}}\Lambda T$ with $\Lambda = \mathrm{diag}\,(0, \lambda_2, \ldots, \lambda_N)$, $T_1 = \frac{1}{\sqrt{N}}1_N \in \mathbb{R}^N$, and $T_{-1} \in \mathbb{R}^{N\times N-1}$. Define the orthogonal transformation of $\tilde{P}$, $\tilde{\xi}$ and $\tilde{\nu}$ by T as: $P_o = \left(P_{o1}, {P_{o-1}}^{\mathrm{T}}\right)^{\mathrm{T}} = [T_1, T_{-1}]^{\mathrm{T}}\tilde{P}$, $\xi_o = \left(\xi_{o1}, {\xi_{o-1}}^{\mathrm{T}}\right)^{\mathrm{T}} = [T_1, T_{-1}]^{\mathrm{T}}\tilde{\xi}$, and $\nu_o = \left(\nu_{o1}, {\nu_{o-1}}^{\mathrm{T}}\right)^{\mathrm{T}} = [T_1, T_{-1}]^{\mathrm{T}}\tilde{\nu}$, then

$$\dot{P}_{o1} = \omega(t)(-T_1^{\mathrm{T}}g + \xi_{o1}), \tag{43a}$$

$$\dot{\xi}_{o1} = -\omega(t)P_{o1}, \tag{43b}$$

$$\dot{\nu}_{o1} = 0, \tag{43c}$$

and

$$\dot{P}_{o-1} = \omega(t)(-T_{-1}^{\mathrm{T}}g + \xi_{o-1}), \tag{44a}$$

$$\dot{\xi}_{o-1} = -\omega(t)\left(T_{-1}^{\mathrm{T}}\mathcal{L}T_{-1}\xi_{o-1} + T_{-1}^{\mathrm{T}}\mathcal{L}T_{-1}\nu_{o-1} + P_{o-1}\right), \tag{44b}$$

$$\dot{\nu}_{o-1} = \omega(t)T_{-1}^{\mathrm{T}}\mathcal{L}T_{-1}\xi_{o-1}. \tag{44c}$$

Construct a positive definite function as follows:

$$\begin{aligned}\mathcal{V}(t) = {} & \frac{a}{2}P_o^{\mathrm{T}}P_o + \frac{a}{2}\xi_o^{\mathrm{T}}\xi_o + \frac{a+b}{2}\nu_{o-1}^{\mathrm{T}}\nu_{o-1} \\ & + \frac{b}{2}(\xi_{o-1} - \nu_{o-1})^{\mathrm{T}}(\xi_{o-1} - \nu_{o-1}) \\ & + \frac{c}{2}(P_o - \xi_o)^{\mathrm{T}}(P_o - \xi_o).\end{aligned} \tag{45}$$

Let $\psi = (P_o^{\mathrm{T}}, \xi^{\mathrm{T}}, \nu^{\mathrm{T}})^{\mathrm{T}}$, then

$$\frac{a}{2}P_o^{\mathrm{T}}P_o \le \mathcal{V}(t) \le \frac{a+3b+2c}{2}\|\psi\|^2. \tag{46}$$

Take the time derivative of (45) along (43)–(44), then

$$\begin{aligned}\dot{\mathcal{V}}(t) = {} & aP_o^{\mathrm{T}}\dot{P}_o + a\xi_o^{\mathrm{T}}\dot{\xi}_o + (a+b)\nu_{o-1}^{\mathrm{T}}\dot{\nu}_{o-1} \\ & + b(\xi_{o-1} - \nu_{o-1})^{\mathrm{T}}(\dot{\xi}_{o-1} - \dot{\nu}_{o-1}) \\ & + c(P_o - \xi_o)^{\mathrm{T}}(\dot{P}_o - \dot{\xi}_o) \\ \le {} & a\omega(t)\left(-\tilde{P}^{\mathrm{T}}g - \lambda_2\xi_{o-1}^{\mathrm{T}}\xi_{o-1}\right) \\ & + b\omega(t)\left(-\xi_{o-1}^{\mathrm{T}}P_{o-1} - \lambda_2\nu_{o-1}^{\mathrm{T}}\nu_{o-1} - \nu_{o-1}^{\mathrm{T}}P_{o-1}\right) \\ & + c\omega(t)\left(-\tilde{P}^{\mathrm{T}}g + P_{o-1}^{\mathrm{T}}\left(T_{-1}^{\mathrm{T}}\mathcal{L}T_{-1}\right)\xi_{o-1}\right. \\ & \quad + P_{o-1}^{\mathrm{T}}\left(T_{-1}^{\mathrm{T}}\mathcal{L}T_{-1}\right)\nu_{o-1} + P_o^{\mathrm{T}}P_o + \xi_o^{\mathrm{T}}Tg \\ & \quad \left.-\xi_o^{\mathrm{T}}\xi_o - \lambda_2\xi_{o-1}^{\mathrm{T}}\xi_{o-1} - \xi_{o-1}^{\mathrm{T}}\left(T_{-1}^{\mathrm{T}}\mathcal{L}T_{-1}\right)\nu_{o-1}\right)\end{aligned} \tag{47}$$

From ((37)a),

$$-\tilde{P}^{\mathrm{T}}g \le -\zeta_\iota^m P_o^{\mathrm{T}}P_o, \tag{48}$$

where $\zeta_\iota^m = \min\{\frac{2a_i}{\bar{\iota}_i^2}\}$. From ((37)b),

$$\xi_o^{\mathrm{T}}Tg \le \frac{1}{2}\xi_o^{\mathrm{T}}\xi_o + \frac{\zeta_\iota^M}{2}P_o^{\mathrm{T}}P_o, \tag{49}$$

where $\zeta_\iota^M = \max\{(\frac{2(a_i+\mu)+\frac{\mu}{\tau}}{\bar{\iota}_i^2})^2\}$. Based on Young's inequality,

$$\begin{aligned}\dot{\mathcal{V}}(t) \le {} & -\omega(t)J_P P_o^{\mathrm{T}}P_o - \frac{c}{2}\omega(t)\xi_o^{\mathrm{T}}\xi_o - \omega(t)J_\nu\nu_{o-1}^{\mathrm{T}}\nu_{o-1} \\ & - \omega(t)J_\xi\xi_{o-1}\xi_{o-1},\end{aligned} \tag{50}$$

where

$$J_P(a) = a\zeta_\iota^m - b^2 + c\left(\zeta_\iota^m - 1 - \frac{\zeta_\iota^M}{2} - \lambda_N^2\right), \tag{51a}$$

$$J_\nu(b) = b\lambda_2 - \frac{1}{2} - c, \tag{51b}$$

$$J_\xi(a) = a\lambda_2 - \frac{1}{2} + c\left(\lambda_2 - \frac{\lambda_N^2}{2} - \frac{1}{2}\right). \tag{51c}$$

Choose b to ensure $J_\nu \ge \frac{c}{2}$, then select a to guarantee $J_P \ge \frac{c}{2}$ and $J_\xi \ge 0$. Then,

$$\begin{aligned}\dot{\mathcal{V}}(t) & \le -\frac{c}{2}\omega(t)\|\psi\|^2 \\ & \le -k_{\mathcal{V}}\omega(t)\mathcal{V}(t) \\ & \le -k_{\mathcal{V}}(r_1 + \frac{r_2}{t_a}\Omega(t))\mathcal{V}(t),\end{aligned} \tag{52}$$

where $k_{\mathcal{V}} = \frac{c}{a+3b+2c}$.

(1) If $t \in [0, t_a)$, from the definition of $\Omega(t)$,

$$\frac{d\Omega(t)^{r_2k_{\mathcal{V}}}}{dt} = \frac{r_2k_{\mathcal{V}}}{t_a}\Omega(t)^{r_2k_{\mathcal{V}}+1}. \tag{53}$$

Multiply $\Omega(t)^{r_2k_{\mathcal{V}}}$ on (52),

$$\Omega(t)^{r_2k_{\mathcal{V}}}\dot{\mathcal{V}}(t) \le -k_{\mathcal{V}}\Omega(t)^{r_2k_{\mathcal{V}}}(r_1 + \frac{r_2}{t_a}\Omega(t))\mathcal{V}(t). \tag{54}$$

From (53) and (54),

$$\frac{d[\Omega(t)^{r_2k_{\mathcal{V}}}\mathcal{V}(t)]}{dt} \le -r_1k_{\mathcal{V}}\Omega(t)^{r_2k_{\mathcal{V}}}\mathcal{V}(t). \tag{55}$$

Then,

$$\mathcal{V}(t) \le e^{-r_1k_{\mathcal{V}}t}\Omega(t)^{-r_2k_{\mathcal{V}}}\mathcal{V}(0). \tag{56}$$

Note that $\lim_{t\to t_a}\Omega(t)^{-r_2k_{\mathcal{V}}} = 0$, then

$$0 \le \lim_{t\to t_a}\mathcal{V}(t) \le 0. \tag{57}$$

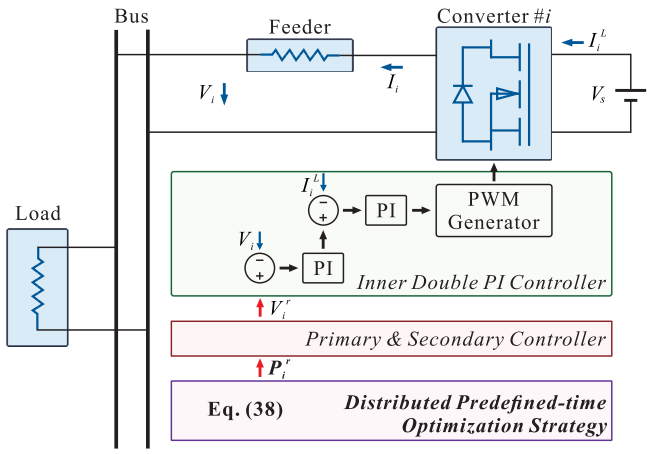

Fig. 2. The hierarchical framework of a microgrid.

Therefore, $\lim_{t\to t_a}\|P^r(t)-P^{rs}\|=0$, $P^r(t)$ in the distributed predefined-time optimization strategy (38) converges to P^*_ϵ within the predefined settling time t_a.

(2) If $t\in[t_a,\infty)$, from (52) and the definition of $\Omega(t)$,

$$\dot{\mathcal{V}}(t)\le -k_{\mathcal{V}}(r_1+\frac{r_2}{t_a})\mathcal{V}(t), \tag{58}$$

then

$$\begin{aligned}\mathcal{V}(t)&\le e^{-k_{\mathcal{V}}(r_1+\frac{r_2}{t_a})(t-t_a)}\mathcal{V}(t_a)\\&\le 0,\end{aligned} \tag{59}$$

which implies $\|P^r(t)-P^{rs}\|=0, t\in[t_a,+\infty)$.

According to (4), the reference generation power $P^r(t)$ in the optimization strategy (38) converges to the $\Delta\epsilon$-feasible suboptimal solution P^*_ϵ within the predefined settling time t_a. □

The time-based function $\Omega(t)$ plays a decisive role in ensuring the predefined-time stability of the system. However, when $t\to t_a$, $\Omega(t)\to\infty$ results in numerical overflow issues in numerical implementation. Thus, a gain limit $\bar{\Omega}$ is required during the implementation of the proposed strategy. Note that $\lim_{t\to t_a}\|P^r(t)-P^{rs}\|$ can be made arbitrarily small by choosing large enough $\bar{\Omega}$. Note that the proposed distributed predefined-time strategy (38) will be implemented in a digital way instead of in hardware in real applications, therefore, $\bar{\Omega}$ can be chosen as large as the software can tolerate.

The hierarchical framework of the optimization strategy is shown for practical application in Fig. 2, where the double PI controller is employed to achieve the fast-tracking of the grid-forming converter output voltage to the reference signal from primary and secondary controllers. The distributed predefined-time optimization strategy is deployed in the tertiary layer to ensure the economic work of the microgrid.

Remark 4.1. Compared with the finite-time optimization strategy in Mao et al. (2021), Zhao and Ding (2018) and the fixed-time optimal dispatch approach in Chen and Guo (2022), Wang et al. (2020) and Liu and Yang (2023), the reference generation power can converge within a predefined settling time, which can be regulated by one parameter t_a. This makes the convergence time of the system states very convenient to adjust. Compared with Guo and Chen (2022a, 2022b), the optimization goal includes not only the power balance but also the transmission loss to match the actual application scenario.

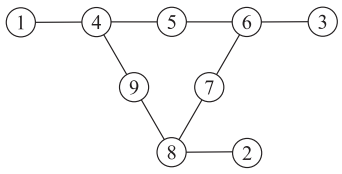

Fig. 3. Grid topology of IEEE 9-bus system.

Table 1
Modified IEEE 9-bus system.

Node	a	b	c	P^{u}	P^{l}	ι
1	0.30	10	5	250	10	0.051
2	0.20	15	10	300	10	0.080
3	0.15	30	5	150	10	0.045
4	0.45	5	0	250	20	0.078
5	0.23	25	14	380	50	0.073
6	0.33	40	5	275	30	0.105
7	0.35	10	20	280	10	0.085
8	0.15	30	2	300	20	0.073
9	0.20	10	17	270	20	0.062

5. Simulation results

In this section, the effectiveness of the distributed predefined-time optimal economic dispatch strategy is verified by a modified IEEE 9-bus system, whose grid topology is shown in Fig. 3. The generation cost and transmission loss parameters are listed in Table 1 with $\tau=0.01$. $P_{L,i}=100$ and $\iota_{L,i}=0.05, i=1,\ldots,N$ with the number of DGs N being 9. The optimization parameters r_1 and r_2 in (38) can be chosen arbitrarily, $\bar{\Omega}$ need to be large to ensure the predefined-time stability. For the predefined settling time parameter $t_a=0.1$, the optimization parameters are set as $r_1=1$ and $r_2=10$ with $\bar{\Omega}=300$. Based on the grid topology in Fig. 3 and the transmission loss coefficients in Table 1 to determine a_{ij} in $\mathcal{L}$, the network parameter $\lambda_2(\mathcal{L})$ equals to 0.68. The proposed optimal economic dispatch strategy is tested by the following cases: effectiveness verification, load change and plug-and-play, topology reconfiguration, and comparison with the existing results.

5.1. Case I : Validity verification

In this case, the effectiveness of the proposed distributed predefined-time optimization strategy is verified. Moreover, the suboptimal generation cost from (38) is compared with the optimization result obtained by the CVX optimization tool. The generation power, gradient, and generation cost are shown in Fig. 4. The comparative optimization results from the proposed strategy and CVX tool are shown in Table 2.

From Fig. 4, the gradient and generation power converge within the predefined settling time 0.1 s, which illustrates the validity of the proposed distributed predefined-time optimization strategy.

From Table 2, under the conditions of power balance equality constraints and generation inequality constraints, the generation cost obtained from (38) is close to that from the CVX optimization tool with an optimization error of 0.004, which verifies the feasibility of the optimization results from the proposed economic dispatch strategy.

To demonstrate the feasibility and applicability in a more complex and realistic case, the proposed optimization strategy is tested in the modified IEEE 39-bus system.

Table 2
Comparative optimization results.

Power(Node)	P(1)	P(2)	P(3)	P(4)	P(5)	P(6)	P(7)	P(8)	P(9)	Cost
CVX	107.468	143.012	149.839	74.846	103.813	45.822	88.303	142.514	159.044	46 794.634
(38)	107.47	143.01	149.84	74.85	103.81	45.82	88.30	142.51	159.04	46 794.63

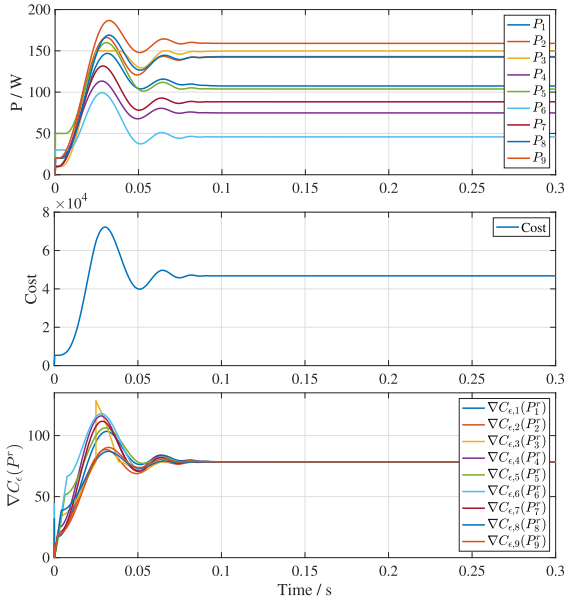

Fig. 4. The validity verification.

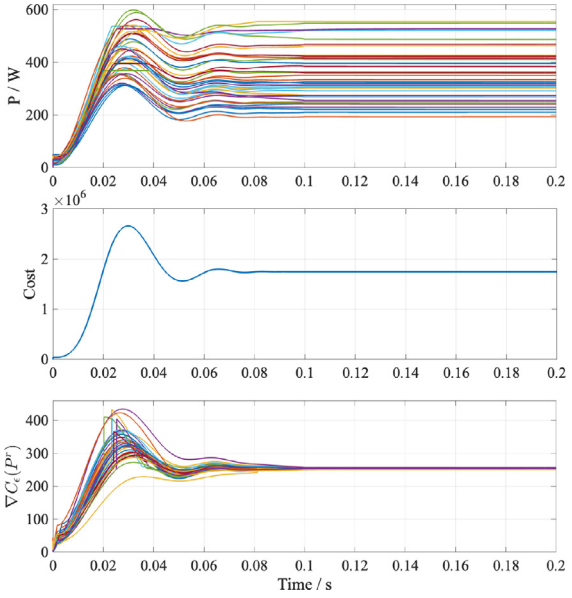

Fig. 5. The validity verification in modified 39-bus system.

From Fig. 5, the gradient and reference power converge within the predefined settling time 0.1 s. Moreover, compared with the optimization results obtained by CVX, the optimization error is within the range of 0.005%. Therefore, the validity and feasibility of the proposed optimization strategy in a more complex and realistic case are illustrated.

5.2. Case II : Impact of parameter changes

In this case, the impact of parameter sensitivity is conducted by changing one of the four optimization parameters (r_1, r_2, t_a, and τ) at a time. Specifically, the optimization parameters are set as $r_1 = 50$, $r_2 = 20$, $t_a = 0.2$, and $\tau = 0.1$ under $P_6^{\mathrm{u}} = 200$ and $P_6^{\mathrm{l}} = 60$ for comparison with the original values.

From Fig. 6, the convergence rates of the reference powers and gradients increase as r_1 changes from 1 to 50 and r_2 changes from 10 to 20 respectively, which verifies the theoretical result in (56). The upper bound of the convergence time of the reference generation power changes according to the change of the predefined-time parameter t_a, which verifies Theorem 4.1. Moreover, compared with the optimization error under $\tau = 0.1$, the optimization error under $\tau = 0.01$ decreases by 0.348, which demonstrates the instruction in Remark 3.2.

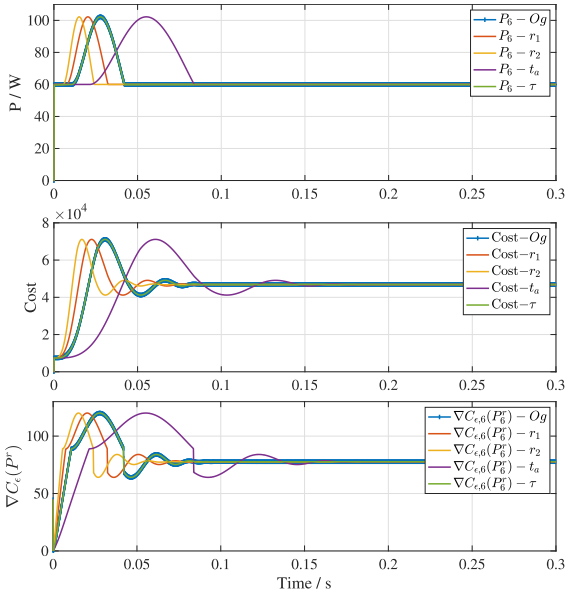

Fig. 6. The impact of parameter changes.

5.3. Case III : Load change and plug-and-play

The effectiveness of the distributed predefined-time strategy in load change and plug-and-play scenarios is verified. At $t = 0.5$ s, the load $P_{L,5}$ changes from 100 W to 150 W. Moreover, the 3rd DG quits working at $t = 1$ s and revises at $t = 1.5$ s.

From Fig. 7, after the load changes, the reference generation power increases to meet the supply–demand power balance while minimizing the generation cost under generation power limits in the microgrid. When the 3rd DG stops working or restarts, the predefined-time optimal economic power dispatch converges to the steady state within the predefined settling time, and both the gradient and generation power converge within 0.1 s to achieve the optimization goals.

5.4. Case IV : Topology reconfiguration

In this case, the effectiveness of the proposed optimization strategy is demonstrated in the scenario of topology reconfiguration. At $t = 2$ s, the line between the 4th and the 5th DG

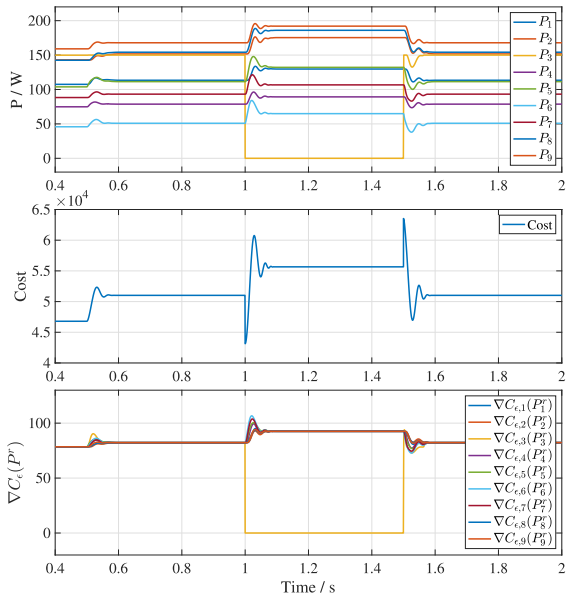

Fig. 7. Load change and plug-and-play tests.

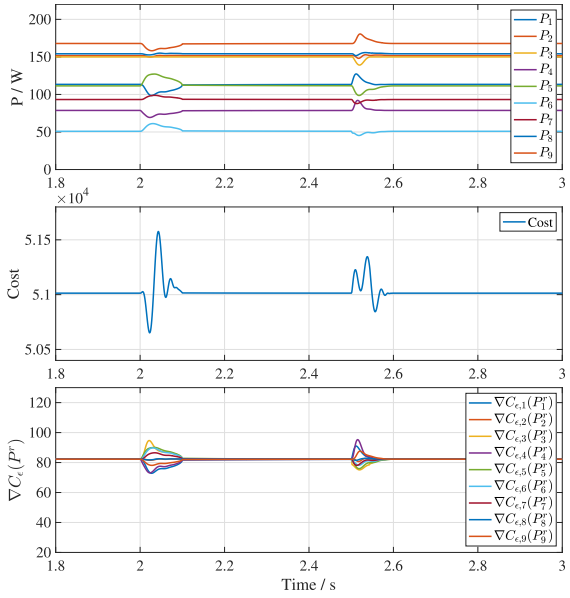

Fig. 8. Topology reconfiguration.

quits running, which means the ring topology is broken in the microgrid. At $t = 2.5$ s, the 1st DG is linked with the 6th DG, which represents another ring is built. With the topology reconfiguration, the network parameter $\lambda_2(\mathcal{L})$ changes to 0.25 at $t = 2$ s and 0.64 at $t = 2.5$ s.

From Fig. 8, after the topology reconfiguration, the system states converge to the steady state within 0.1 s, which illustrates the effectiveness of the optimal economic dispatch strategy in the topology reconstruction scenario.

5.5. Case V : Comparative simulation

In this case, the proposed predefined-time optimal economic dispatch strategy is compared with the finite-time optimization approach in Zhao and Ding (2018), the fixed-time optimal dispatch scheme in Liu and Yang (2023) and the predefined-time

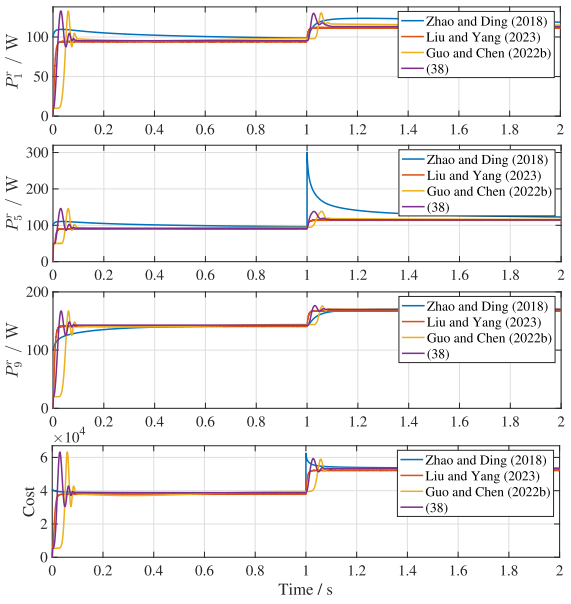

Fig. 9. Comparative results.

resource allocation method in Guo and Chen (2022b). The finite-time optimization gain parameters in Zhao and Ding (2018) are set as $p = 1$ and $q = 11$ to minimize the upper bound of the convergence time. According to the parameter τ and $\overline{P}^{\text{ul}}$, a large penalty function parameter ϵ value is obtained, which does not match the practical application. Thus, the parameter ϵ is chosen as 3.3. The fixed-time optimal dispatch gain parameters in Liu and Yang (2023) are set as $k_1 = k_2 = 24$ and $\xi = 1$ so that the upper bound of the convergence time is equal to 0.1 s. The parameters α and k_3 are chosen as 100 and 10000 to approach the power balance equality constraint. For the predefined-time resource allocation parameters in Guo and Chen (2022b), the predefined time parameter t_f is set to be the same as t_a. The optimization gains are arbitrarily chosen as $\sigma = 0.1$ and $\vartheta = 5$ with $\epsilon = 3.3$. The load $P_{L,5}$ increases by 200 W at $t = 1$ s. ι_i and $\iota_{L,i}$, $i = 1, \ldots, N$ are set to 0 for the comparison with the methods in Guo and Chen (2022b), Zhao and Ding (2018), which means no consideration of transmission loss. The dynamic reference power and the generation cost are shown in Fig. 9.

From Fig. 9, the convergence rate of the system states under the proposed distributed predefined-time optimal economic dispatch strategy is faster than that under the finite-time optimal dispatch in Zhao and Ding (2018). Compared with Liu and Yang (2023), an accurate power balance equality constraint is satisfied under the proposed strategy. Compared with the allocation method in Guo and Chen (2022b), the system states under the proposed strategy converge to a suboptimal solution closer to the optimal one within 0.1 s. From Fig. 9, after the load changes at $t = 1$ s, it obtains that the proposed strategy can ensure faster convergence speed and get nearer optimal results in the load-switching scenario.

6. Experimental verification

In this section, the experiment verification is executed on a hardware-in-the-loop platform as shown in Fig. 10. The experimental platform consists of IT6724H DC Power Supply (output voltage: 0–300 V, output current: 0–10 A, output power: 0–1500 W, resolution: 100 mV/10 mA), dSPACE 1202, boost

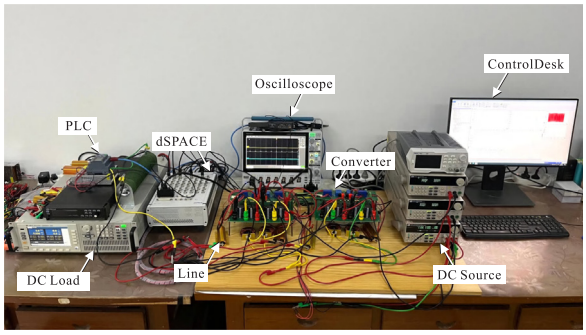

Fig. 10. Microgrid experiment platform.

Table 3
Modified IEEE 4-bus DC microgrid.

Node	a	b	c	P^{u}	P^{l}	$\iota(10^{-3})$
1	0.15	5	5	20	5	9.375
2	0.10	10	5	60	15	4.125
3	0.20	3	10	40	5	9.375
4	0.18	4	8	40	5	4.125

converter (inductance: 2 mH, capacitance: 1 mF, switching frequency: 10 kHz), IT8615 DC Electronic Load (input voltage: 10–600 V, input current: 0.1–20 A, input power: 0–1800 W), resistive transmission lines, MSO46 Oscilloscope, PLC, and desktop computer.

The microgrid topology is modified from IEEE 4-bus system, and the generation cost and transmission loss parameters are listed in Table 3 with $\tau = 0.1$. $P_{L,i} = 20$ and $\iota_{L,i} = 0, i = 1, \ldots, N$ with the number of DGs N being 4. For the predefined settling time parameter $t_a = 1$, the optimization parameters are set as $r_1 = 1$ and $r_2 = 10$ with $\bar{\Omega} = 10$. Based on the ring grid topology of 1-2-3-4(-1) and the transmission loss coefficients, the network parameter $\lambda_2(\mathcal{L})$ equals to 23.4. The proposed optimal economic dispatch strategy is tested by the following cases: load change, plug-and-play, and comparative experiment with the existing result.

6.1. Case I : Validity verification and load change

In this case, the effectiveness of the proposed distributed predefined-time optimal economic dispatch strategy is verified. Moreover, the load $P_{L,i}$ changes from 20 W to 30 W at $t = 15$ s. The output power, gradient, and generation cost are shown in Fig. 11.

From Fig. 11, the output power and the gradients converge within the predefined settling time 1 s, which illustrates the validity of the proposed distributed predefined-time optimal economic dispatch strategy. After the load demand increases, DGs generate more power to meet the power balance while achieving the minimization of the generation cost with transmission loss under generation limits.

6.2. Case II : Plug-and-play

In this case, the plug-and-play performance of the distributed predefined-time optimal economic dispatch strategy is tested. The 1st DG quits working at $t = 25$ s and revises at $t = 35$ s.

From Fig. 12, when the 1st DG stops working and restarts, the output power and gradient converge to the steady state within 1 s, and the minimization of the generation cost with transmission loss is realized under equality and inequality constraints.

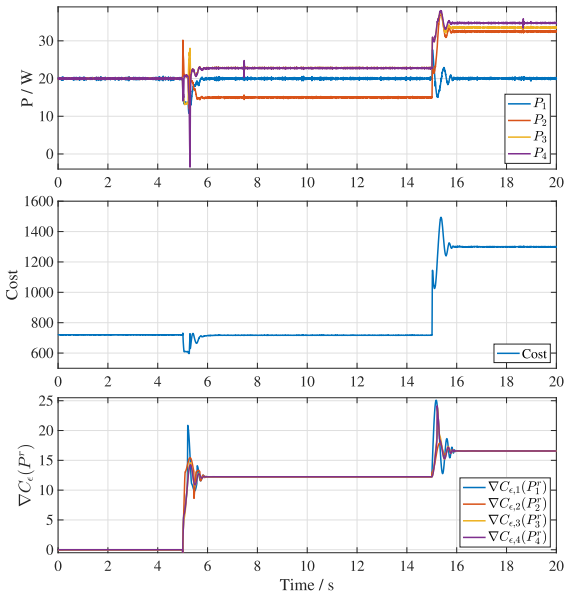

Fig. 11. Validity verification and load change.

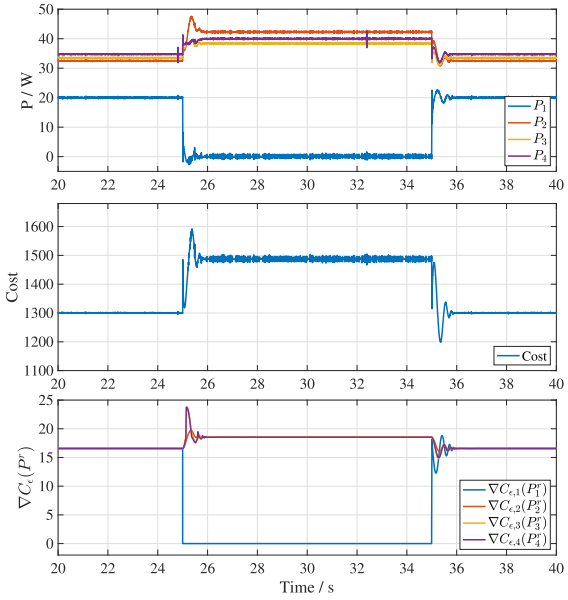

Fig. 12. Plug-and-play.

6.3. Case III : Comparative experiment

In this case, the proposed distributed predefined-time optimal economic dispatch strategy is compared with the predefined-time resource allocation approach in Guo and Chen (2022b). For the optimization parameters in Guo and Chen (2022b), the predefined settling time parameter t_f is set to be the same as t_a to guarantee the same upper bound of the convergence time. The optimization gains are arbitrarily chosen as $\sigma = 0.1$ and $\vartheta = 4$ with $\epsilon = 1$. The load $P_{L,i}$ increases by 10 W at $t = 15$ s. The output power and the generation cost are shown in Fig. 13.

From Fig. 13, compared with the allocation strategy in Guo and Chen (2022b), the system states under the proposed strategy converge to the steady state within 1 s. At $t = 10$ s, the generation cost from (38) is 717.1. On the contrary, the generation cost from Guo and Chen (2022b) is 718.3, which means a nearer optimal result is obtained by the proposed strategy. Moreover,

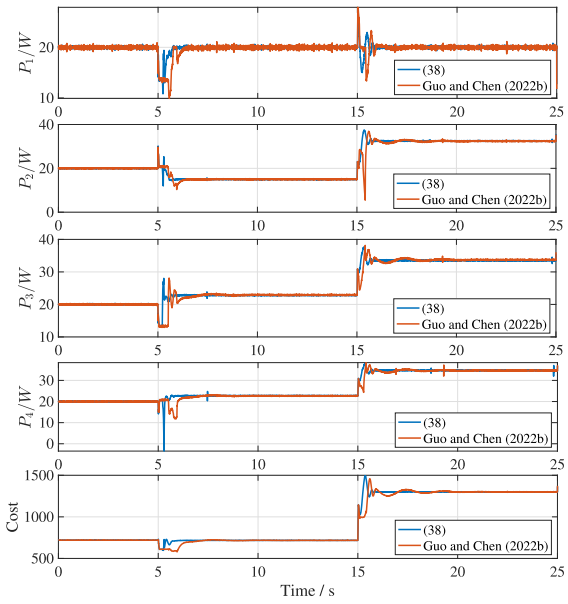

Fig. 13. Comparative results.

from Fig. 13, after the load changes at $t = 15$ s, it can be seen that the proposed power dispatch strategy can obtain a faster convergence rate and nearer optimal results in the load-switching scenario.

7. Conclusion

In this paper, a novel smooth reconstruction penalty function with continuous and piecewise linear differential is designed to deal with generation constraints, which promotes to present a better suboptimal solution. A distributed predefined-time optimal economic dispatch strategy is proposed by employing a time-based function. The minimization of the generation cost with transmission loss under the power balance and generation constraints can be realized within a predefined settling time. The proposed optimization strategy is tested by simulations and hardware-in-the-loop experiments to illustrate the advantages of fast convergence rate and near optimal solution. Future work could focus on predefined-time optimization under cyber attack in a microgrid.

References

Becerra, H. M., Vázquez, C. R., Arechavaleta, G., & Delfin, J. (2018). Predefined-time convergence control for high-order integrator systems using time base generators. *IEEE Transactions on Control Systems Technology*, *26*(5), 1866–1873.

Bertsekas, D. P. (1975). Necessary and sufficient conditions for a penalty method to be exact. *Mathematical Programming*, *9*(1), 87–99.

Binetti, G., Davoudi, A., Lewis, F. L., Naso, D., & Turchiano, B. (2014). Distributed consensus-based economic dispatch with transmission losses. *IEEE Transactions on Power Systems*, *29*(4), 1711–1720.

Chen, G., & Guo, Z. (2022). Initialization-free distributed fixed-time convergent algorithms for optimal resource allocation. *IEEE Transactions on Systems, Man, and Cybernetics: Systems*, *52*(2), 845–854.

Cherukuri, A., & Cortés, J. (2018). Distributed coordination of DERs with storage for dynamic economic dispatch. *IEEE Transactions on Automatic Control*, *63*(3), 835–842.

Chiang, C.-L. (2005). Improved genetic algorithm for power economic dispatch of units with valve-point effects and multiple fuels. *IEEE Transactions on Power Systems*, *20*(4), 1690–1699.

Dragičević, T., Lu, X., Vasquez, J. C., & Guerrero, J. M. (2016). DC microgrids–Part II: A review of power architectures, applications, and standardization issues. *IEEE Transactions on Power Electronics*, *31*(5), 3528–3549.

Gaing, Z.-L. (2003). Particle swarm optimization to solving the economic dispatch considering the generator constraints. *IEEE Transactions on Power Systems*, *18*(3), 1187–1195.

Guo, Z., & Chen, G. (2022a). Distributed dynamic event-triggered and practical predefined-time resource allocation in cyber–physical systems. *Automatica*, *142*, Article 110390.

Guo, Z., & Chen, G. (2022b). Predefined-time distributed optimal allocation of resources: A time-base generator scheme. *IEEE Transactions on Systems, Man, and Cybernetics: Systems*, *52*(1), 438–447.

Kia, S. S. (2016). Distributed optimal resource allocation over networked systems and use of an e-exact penalty function. *IFAC-PapersOnLine*, *49*(4), 13–18.

Li, Q., Gao, D. W., Zhang, H., Wu, Z., & Wang, F.-Y. (2019). Consensus-based distributed economic dispatch control method in power systems. *IEEE Transactions on Smart Grid*, *10*(1), 941–954.

Liu, X.-K., Wang, Y.-W., Liu, Z.-W., & Huang, Y. (2023). On the stability of distributed secondary control for DC microgrids with grid-forming and grid-feeding converters. *Automatica*, *155*, Article 111164.

Liu, L.-N., & Yang, G.-H. (2023). Distributed fixed-time optimal resource management for microgrids. *IEEE Transactions on Automation Science and Engineering*, *20*(1), 404–412.

Liu, H., Zheng, W. X., & Yu, W. (2021). Distributed discrete-time algorithms for convex optimization with general local constraints on weight-unbalanced digraph. *IEEE Transactions on Control of Network Systems*, *8*(1), 51–64.

Mao, S., Dong, Z., Schultz, P., Tang, Y., Meng, K., Dong, Z. Y., & Qian, F. (2021). A finite-time distributed optimization algorithm for economic dispatch in smart grids. *IEEE Transactions on Systems, Man, and Cybernetics: Systems*, *51*(4), 2068–2079.

Pinar, M. Ç., & Zenios, S. A. (1994). On smoothing exact penalty functions for convex constrained optimization. *SIAM Journal on Optimization*, *4*(3), 486–511.

Schiffer, J., Zonetti, D., Ortega, R., Stanković, A. M., Sezi, T., & Raisch, J. (2016). A survey on modeling of microgrids—From fundamental physics to phasors and voltage sources. *Automatica*, *74*, 135–150.

Shao, S., Liu, X., & Cao, J. (2021). Prespecified-time synchronization of switched coupled neural networks via smooth controllers. *Neural Networks*, *133*, 32–39.

Shuai, H., Fang, J., Ai, X., Tang, Y., Wen, J., & He, H. (2019). Stochastic optimization of economic dispatch for microgrid based on approximate dynamic programming. *IEEE Transactions on Smart Grid*, *10*(3), 2440–2452.

Wang, X., Wang, G., & Li, S. (2020). A distributed fixed-time optimization algorithm for multi-agent systems. *Automatica*, *122*, Article 109289.

Wood, A. J., Wollenberg, B. F., & Sheblé, G. B. (2013). *Power generation, operation, and control*. John Wiley & Sons.

Xu, Y., & Li, Z. (2015). Distributed optimal resource management based on the consensus algorithm in a microgrid. *IEEE Transactions on Industrial Electronics*, *62*(4), 2584–2592.

Yang, S., Tan, S., & Xu, J.-X. (2013). Consensus based approach for economic dispatch problem in a smart grid. *IEEE Transactions on Power Systems*, *28*(4), 4416–4426.

Zhao, T., & Ding, Z. (2017). Distributed initialization-free cost-optimal charging control of plug-in electric vehicles for demand management. *IEEE Transactions on Industrial Informatics*, *13*(6), 2791–2801.

Zhao, T., & Ding, Z. (2018). Distributed finite-time optimal resource management for microgrids based on multi-agent framework. *IEEE Transactions on Industrial Electronics*, *65*(8), 6571–6580.

Yu Zhang received the B.S. degree from Taiyuan University of Technology, Taiyuan, China, in 2020. He is currently working toward the Ph.D. degree in control theory and control engineering with the Huazhong University of Science and Technology, Wuhan, China. His research interests include multi-agent systems, distributed control and optimization, and hybrid microgrids.

Yan-Wu Wang received the B.S. degree in automatic control, the M.S. degree and the Ph.D. degree in control theory and control engineering from Huazhong University of Science and Technology (HUST), Wuhan, China, in 1997, 2000, and 2003, respectively. She has been a Professor with the School of Artificial Intelligence and Automation, HUST, since 2009. Currently, she is also with the Key Laboratory of Image Processing and Intelligent Control, Ministry of Education, China. Her research interests include hybrid systems, cooperative control, and multi-agent systems with applications in the smart grid.

Dr. Wang was a recipient of several awards, including the first prize of Hubei Province Natural Science in 2014, the first prize of the Ministry of Education of China in 2005, and the Excellent Ph.D. Dissertation of Hubei Province in 2004,

China. In 2008, she was awarded the title of "New Century Excellent Talents" by the Chinese Ministry of Education.

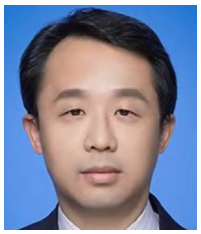

Jiang-Wen Xiao received the B.S. degree in electrical engineering, the M.S. degree in control theory and control engineering, and the Ph.D. degree in systems engineering from the Huazhong University of Science and Technology (HUST), Wuhan, China, in 1994, 1997, and 2001, respectively. He is currently a Professor with the School of Artificial Intelligence and Automation, HUST, where he is also with the Key Laboratory of Image Processing and Intelligent Control, Ministry of Education, China. His research interests include smart grid technologies and power markets.

Xiao-Kang Liu received the B.S. degree in automatic control and the Ph.D. degree in control science and engineering from Huazhong University of Science and Technology (HUST), Wuhan, China, in 2014 and 2019, respectively. From Jul. 2017 to Aug. 2018, he was a visiting scholar with the Department of Electrical, Computer, and Biomedical Engineering, University of Rhode Island, RI, USA. From Oct. 2019 to Feb. 2021, he was a postdoctoral research fellow with the School of Electrical & Electronic Engineering, Nanyang Technological University (NTU), Singapore. He is currently an Associate Professor with the School of Artificial Intelligence and Automation, HUST. His research interests include hybrid control, distributed control and optimization, DC microgrids.